Graphene-based supercapacitor with carbon nanotube film as a highly efficient current collector

Marco Notarianni[1], Jinzhang Liu[1], Francesca Mirri[2], Matteo Pasquali[2] and Nunzio Motta[1]

[1]Institute for Future Environments and School of Chemistry, Physics, and Mechanical Engineering, Queensland University of Technology, Brisbane, 4001 QLD, Australia

[2]Department of Chemical and Biomolecular Engineering, The Smalley Institute for Nanoscale Science and Technology, Rice University, 6100 Main Street, Houston, Texas 77005, United States

E-mail: jinzhang.liu@qut.edu.au and n.motta@qut.edu.au

Abstract

Flexible graphene-based thin film supercapacitors were made using carbon nanotubes (CNTs) films as current collectors and graphene films as electrodes. The graphene sheets were produced by simple electrochemical exfoliation, while the graphene films with controlled thickness were prepared by vacuum filtration. The solid-state supercapacitor was made by using two graphene/CNT films on plastic substrates to sandwich a thin layer of gelled electrolyte. We found that the thin graphene film with thickness <1 μm can greatly increase the capacitance. Using only CNT films as electrodes, the device exhibited a capacitance as low as ~ 0.4 mF/cm^2, whereas by adding a 360-nm-thick graphene film to the CNT electrodes led to a ~ 4.5 mF/cm^2 capacitance. We experimentally demonstrated that the conductive CNT film is equivalent to gold as

current collector while it provides a stronger binding force to the graphene film. Combining the high capacitance of the thin graphene film and the high conductivity of the CNT film, our devices exhibited high energy density (8-14 Wh/kg) and power density (250-450 kW/kg).

Keywords

Supercapacitor; Graphene; Electrochemical exfoliation; Carbon nanotube film; Current collector.

1. Introduction

Electrical energy storage plays an important role in the high tech industry as the energy components are indispensible to portable devices and hybrid vehicles [1, 2]. Supercapacitors have attracted much interest in the last decade and their technology advanced with the use of carbon nanomaterials. The unique features of supercapacitors, such as high power density, ability to charge and discharge within seconds, long lifetime, and no maintenance, make them superior to traditional batteries in practical applications [3, 4]. At the current stage, the energy density of a commercial supercapacitor is still much lower compared to that of a standard battery, however the combination of a supercapacitor with a battery has been the design of choice to power electrical vehicles, exploiting the short duration power boost of a supercapacitor for vehicle acceleration. Today, most supercapacitor manufacturers use coconut shell activated carbon as their active material. Commercial supercapacitors are bulky and require high standard encapsulation to avoid the leakage of liquid electrolyte. The development of gel polymer electrolytes allows for the fabrication of solid-state supercapacitors, simplifying the

fabrication process and making this technology very appealing for several applications [5, 6]. The use of polymer electrolyte has led to paper-like supercapacitors that can be bent and twisted [7]. Other authors used titania nanotubes as substrate and loaded NiO on top of the nanotube network by anodizing a Ni-Ti binary alloy foil, reporting a high value of areal capacitance (1-10 F/cm^2) [8]. They suggest that the faster charge/discharge kinetics of NT electrodes at high scan rates is due to the ordered NT film architecture. Presumably, the direct conducting pathways for electrons in the NT walls and for ions through the pore -system facilitate t discharge reactions.

Carbon nanomaterials like carbon nanotubes (CNTs) and graphene have been proposed as electrode materials in supercapacitors because of their extraordinary large specific surface area, remarkable chemical stability, high electric conductivity, thermal and mechanical properties [9-13]. They are in fact valid candidates to replace activated carbons that present a low specific capacitance due to a great portion of micropores, leading to low electrode-electrolyte accessibility [14]. The main advantage of CNT and graphene is that they can provide higher conductivity than other carbonaceous materials, leading to a more simple and lightweight device. The combination of gelled electrolyte and thin films of carbon nanomaterials opens opportunities for developing flexible supercapacitors that can be combined with bendable displays and touch-pads.

Supercapacitor electrodes based on CNTs have been made by using either CNT arrays grown on a substrate or network films processed from a CNT suspension [12-15]. For individual CNTs only the outer surface can be used to absorb ions, whereas for a graphene sheet both sides can be exploited to trap ions, making graphene more suitable

for making high-capacitance electrodes. Xu *et al.* prepared a 3D porous structure of reduced graphene oxide (rGO) for electrodes by pressing such thick films onto an Au-coated plastic substrate to make supercapacitors [16]. However, the high cost of using Au as the current collector has to be considered if devices are produced on an industrial scale. El-Kady *et al*. developed a novel technique to thermally reduce GO using the laser of a DVD optical drive and assembling laser-scribed graphene films with gelled electrolyte to make supercapacitors [17, 18]. The conductivity of their graphene film is 1738 S/m, equivalent to 75 Ω/sq (the thickness of laser-irradiated graphene film is 7.6 μm), leading to an increase of the resistance of the device if used as both the electrode and current collector. High internal resistance not only decreases the power density of the device, but also leads to heat problems when charged/discharged at large currents. Hence, a current collector with high conductivity and the ability to bind with the graphene electrode can be helpful in improving the capacitive performance and facilitating the device fabrication. Metal foils such as Al, Cu, and stainless steel with thicknesses between 20 μm and 80 μm are largely used as current collectors in commercial supercapacitors. The metal foil suffers from corrosion due to the use of acidic electrolyte, thus requiring special technique to passivate the metal surface [19]. Zhou *et al* used cross-stacking aligned CNT film as current collector to support metal oxide nanoparticles and made supercapacitors using liquid electrolyte [20]. In their work the sheet resistance of CNT film is 50 Ω/sq.

In this paper we report the use of double-wall CNT (DWCNT) films with very low sheet resistance as current collectors and graphene films as electrodes to make flexible and solid-state supercapacitors. The function of the CNT film is investigated by

comparing it with a gold film used to support the graphene electrode. We studied the dependence of the capacitance on the graphene film thickness, ranging from 50 nm to 360 nm.

2. Experiment

2.1 Preparation of CNT Films

DWCNTs with an average length of 10 μm and average diameter of 2.4 nm were purchased from Continental Carbon Nanotechnologies, Inc. (batch X647H) and mixed with chlorosulfonic acid at 2000 rpm with a speed-mixer (DAC 150.1 FV-K, Flak Tek Inc) for 20 min. In order to make CNTs films, the solution was diluted to 20 ppm and then vacuum filtered by using alumina membranes (Whatman Co., pore size 200 nm). The CNT film on the membrane was washed by chloroform to remove most of the acid (film coagulation) and then dried in air at room temperature overnight [21]. The alumina membrane was etched away by floating it onto an aqueous solution of NaOH (0.5 M) in a petri dish. After draining off the NaOH solution and refilling with DI water, the CNT film was transferred onto a polyethylene naphthalate (PEN) paper and then dried at 50 °C for 5 hours. The CNT film was characterized by Raman spectroscopy and its thickness was optically determined to be 520 nm (Supporting Information), weighting 29 $\mu g/cm^2$. The sheet resistance of the CNTs film measured by a four-point probe meter was 5 Ω/sq.

2.2. Preparation of Graphene Films

Graphene was produced by electrochemically exfoliating highly oriented pyrolytic graphite (1×1 cm^2) in a 150 mL aqueous solution containing 0.15 M Na_2SO_4 and 0.01 M sodium dodecyl sulfate. A Pt wire was used as a cathode and the voltage was set to be

5-6 V. The setup was placed in a sonicator during the electrochemical exfoliation process, which results in a final product consisting of mostly bilayer graphene. By using atomic force microscopy to scan a number of graphene sheets randomly dispersed onto a Mica substrate, statistics of the graphene flake thickness was obtained. Details of the experiment and characterization of graphene samples can be found in our previous work [22, 23].

The graphene sheets dispersed in dimethylformamide (DMF) were vacuum filtered onto a porous alumina membrane (Whatman Co., pore size 100 nm) in order to form a uniform film. The film thickness was controlled by measuring the volume of suspension for filtration. After drying, the membrane covered with the graphene film was etched away with the same process described above for the CNT film. The graphene film was then transferred onto the PEN-supported CNT film and dried at 50 °C in air. For comparison, a graphene film transferred onto Au-coated PEN film was also used to make a device.

2.3. Fabrication of solid-state supercapacitors

Methods for preparing the gel electrolyte are reported by Kaempgen *et al*. [24]. In our case, 1 g of poly(vinyl alcohol) (PVA) was dissolved into 10 mL DI water at 90 °C by continuous stirring. After cooling to room temperature, 0.8 g of H_3PO_4 (85% solution in water) was mixed with the gel by stirring. The plastic substrate coated with carbon nanomaterials was cut into rectangular pieces to make devices. The electrolyte gel was applied on the two electrodes and dried at room temperature for 5 h before stacking the two substrates together face-to-face. The device was then left at room temperature for other 10 h to assure the solidification of the gel electrolyte, which glues the two electrode

films together. The thickness of electrolyte layer is about 15 μm and the capacitor working area is 1 cm^2.

We made three types of supercapacitors (D1, D2, and D3) with different electrodes, as illustrated in figure 1. In D1, the CNT film was used as both current collector and electrode. In D2, the graphene film attached to the CNT film was used as electrode. In D3, the Au film was used to replace the CNT film as current collector.

2. Results and discussions

The CNT films were well attached to the PEN plastic substrates without any binder. Figure 2(a) is an optical photograph showing the plastic substrate coated with carbon nanomaterials used to make the supercapacitors. The graphene film coated onto the CNT film can be easily recognized by naked eye. A tilted-view field-emission scanning electron microscopy (FE-SEM, Zeiss Sigma) image in figure 2(b) shows that the CNT film is felt-like and the graphene film on top has wrinkles. Figure 2(c) shows a free-standing graphene film peeled off the substrate. CNTs stuck to the bottom face indicate a strong binding force at the graphene/CNTs interface, though no use has been made of bonder additives. Presumably, the strong bonding is due to the functional groups of the graphene and the residual sulphuric acid present in the CNT films due to the reaction of chlorosulfonic acid with the moisture of the air. In fact, our graphene, produced by electrochemical exfoliation, contains 13 at. % of C-O and a 3 at. % of C=O functional groups as revealed by X-ray photoelectron spectroscopy [22]. On the other hand, it has been demonstrated that CNTs and graphene sheets in solution are mutually attracted due to the π-π interactions between basal planes [25]. Hence the Van der Waals force is also a factor making the graphene film adhere to the CNT film. Figure 2(d) shows the plane-

158 view SEM image of a CNT film. Bundles of CNTs are interlaced to form a mat-like film
159 used as current collector.
160
161 Devices D1 and D2 were tested and their performance results are compared in figure
162 3. Both devices had 520 nm-thick CNT films coated onto plastic sheets, however D1 had
163 the CNT film as both electrode and current collector, while D2 had an 85-nm-thick
164 graphene film coated onto the CNT film as electrode. Figures 3(a) and 3(b) show the
165 cyclic voltammetry (CV) curves of D1 and D2, respectively. The CV curves measured
166 from -1 V to +1V are quite symmetric and exhibit quasi-rectangular shape. The
167 galvanostatic charge-discharge (CD) curves of D1 and D2, measured at different current
168 values, are shown in figures 3(c) and 3(d), respectively. The CV curves are closer to a
169 rectangular shape and the CD curves are in a symmetric triangle shape. However, when
170 graphene was used as electrode (D2), the CV and CD curves were more distorted
171 compared to those of D1, but gained a much larger current range for the CV loop and
172 longer duration for a CD cycle. This means that the capacitance of D2 is higher than that
173 of D1, due to the graphene film electrode.
174 We made device D3 with a graphene film as electrode and a Au film as current
175 collector. D2 and D3 had identical graphene film electrodes with a thickness of 85 nm,
176 weighing ~35 $\mu g/cm^2$. We found that the adhesion force between the graphene sheets and
177 the Au film is relatively weak as the graphene film can be easily peeled off with a
178 tweezer. The Nyquist impedance spectra of D1, D2, and D3, measured from 0.05 Hz to 1
179 MHz, are shown in figure 4(a) with the high frequency region magnified in the inset. For
180 an ideal capacitor, the impedance plot would be a vertical line and the intercept on Re(Z)

axis would represent the internal resistance of the device. Therefore D1 with only the CNT film on the substrate had the best capacitive behaviour. From the inset, the internal resistance values for D1, D2, and D3 were found to be 78 Ω, 79 Ω, and 40 Ω, respectively. The relative high resistance of D1 and D2 can be attributed to the relatively high sheet resistance of the CNT film (5 Ω/sq) and the contact resistance between the CNT film and the metal clip. For D3, with a highly conductive Au film (in the order of 10^{-4} Ω/sq) as current collector, the internal resistance can be attributed to the graphene film composed of slightly oxidized graphene sheets [22]. The sheet resistance of the CNT film is higher than that of the Au film but lower than that of commercial ITO glass (8-60 Ω/sq) [26]. The variations of phase angle with respect to the scanning frequency are shown in figure 4(b) for the three devices. At low frequencies, the D1 phase angle change was up to -84^{o}, close to the ideal value of -90^{o}. The other two devices, D2 and D3, were relatively inferior in the capacitive behavior, while their capacitance values were much higher due to the use of graphene film, as shown in figure 4(c). The capacitance values were extracted from the CV curves and the dependence of specific capacitance against voltage scan rate was plotted for each device. The decrease of capacitance with the increase of the voltage scan rate is related to the diffusion and response time of ions in the electrolyte. D2 and D3 were almost identical in capacitance, indicating that: (i) the CNT film is as efficient as the Au film for collecting charges from the electrode and (ii) the CNT film does not contribute to the capacitance. At a scan rate of 10 mV/s, the areal capacitance of D1 was 0.6 mF/cm^2, while that of D3 was 2.1 mF/cm^2. This means that the capacitance of an 85-nm-thick graphene film is about 3.5 times larger than that of a ~520-nm-thick CNT film. The areal density of the graphene film was 35 μg/cm^2, and that of the

CNT film was 29 μg/cm^2. Using these values, the mass specific capacitance (F/g) for the three devices were obtained (figure 4(d)).

In order to investigate the relationship of graphene film thickness and capacitance, we made D2 type devices by varying the graphene film thicknesses. From this group of devices we obtained the dependence of capacitance against graphene film thickness, as shown in figure 5. Overall, the thicker the graphene film, the higher the areal specific capacitance. In fact, by adding more graphene sheets, more ions can be stored in the electrode. However, the mass specific capacitance decreases when the graphene film thickness is increased from 100 nm to 360 nm. Charging the capacitor means driving ions from the electrolyte into the stacked graphene sheets. Graphene sheets at the bottom of a thick electrode are not fully exploited to trap ions, thus the mass specific capacitance of thick graphene films is low when compared to that of a thin graphene films. The laser-scribe graphene film produced by El-Kady *et al*. was about 7.6 μm-thick and the areal capacitance was ~5 mF/cm^2 [17]. In our work, the 0.36 μm-thick graphene film shows a capacitance of 4.3 mF/cm^2. The areal capacitance could be increased by increasing the graphene film thickness. However, as described in the experimental section, the graphene film is transferred from the water surface to the CNT film; graphene films over a certain thickness will contract and detach off the CNT film during the drying process. Having a thin graphene film with high capacitance is important to achieve high volumetric energy density, especially for a paper-like supercapacitor made by stacking a number of thin film supercapacitor units. Figure 5(b) shows the stability of a D2 device with 85 nm-thick graphene films, which was tested by repeatedly charging and discharging the device at 25 μA/cm^2 for five days. The device retained 89% of its initial capacitance after the stability

test. In fact, the device stability is related to the charge-discharge rate and the electrolyte. The capacitance would be even more stable if the device was tested with a higher charge/discharge current, which corresponds to shorter cycle period. Furthermore, the stability could be improved if gelled ionic liquid is used as electrolyte [27, 28].

Energy and power densities of three devices, one D1 with only CNT films and two D2 with graphene films in different thicknesses, are shown in figure 6. For comparison, also the power and energy densities of Li ion thin film battery and previously reported supercapacitor based on laser-scribed graphene are shown. In figure 6(a), the device with 360-nm-thick graphene film has the highest volumetric energy density (~10^{-4} Wh/cm^3), which is close to the energy density of Li ion film battery (10^{-4}-10^{-3} Wh/cm^3) [28]. Mass energy and power densities of the three devices are shown in figure 6(b). The device with 85-nm-thick graphene films has the highest values in terms of mass power and energy densities. Its power density is in the range of 250-450 kW/kg and the energy density range is 8-14 Wh/kg. Xu *et al*. used ~120-μm-thick porous graphene film and gelled electrolyte to make supercapacitors which showed very high areal specific capacitance up to 400 mF/cm^2 [16]. The values of energy and power densities as a function of mass, reported in that work, are represented by the green region in figure 6(b). The power density (0.5-5.0 kW/kg) is about 100 times lower than that of our D2 device with 85 nm-thick graphene films. The combination of a CNTs film and a graphene film, with total thickness <1 μm when stacked together, has the potential to make thin film supercapacitors with volumetric energy densities comparable to that of a Li film battery. In our work, the electrochemically produced graphene sheets are compactly stacked to

form thin films. We believe that the capacitance can be further improved if the film is processed to be rough and porous.

3. Conclusion

We fabricated solid-state electrochemical supercapacitors using graphene films as electrodes and CNTs films as current collectors. Thin films of carbon nanomaterials were supported by plastic papers which make the device bendable. By comparing different types of devices, we concluded that thin graphene films, made by filtration of electrochemically-produced graphene sheets, have much higher capacitance than the mat-like CNT films. For supercapacitor application, CNT films are comparable to Au films when used as current collectors and are superior to Au films in providing strong adhesion to the graphene electrodes. We investigated the relationship of specific capacitance and graphene film thickness. The areal specific capacitance can be improved by increasing the electrode thickness, and 4.3 mF/cm^2 was achieved by using a 360-nm-thick graphene film as electrode. Our study suggests that the combination of CNT films and graphene films is very suitable for making paper-like supercapacitors with the graphene/CNT bilayer film < 1 μm in thickness while maintaining high energy and power densities.

Acknowledgements

The authors acknowledge the financial support of the Australian Research Council through the Discovery Projects DP130102120 and DP110101454. We also acknowledge the QUT Vice-Chancellor's Research Fellowship and the Marie Curie International Research Staff Exchange Scheme Fellowship within the 7th European Community Framework Programme.

This work was performed in part at the Queensland node of the Australian National Fabrication Facility (ANFF) - a company established under the National Collaborative Research Infrastructure Strategy to provide nano and microfabrication facilities for Australia's researchers.

References

[1] Liu C, Li F, Lai-Peng M and Cheng H M 2010 Advanced materials for energy storage *Adv. Mater.* **22** 28-62

[2] Karden E, Ploumen S, Fricke B, Miller T and Snyder K 2007 Energy storage devices for future hybrid electric vehicles *J. Power Sources* **168** 2-11

[3] Yu A, Davies A and Chen Z 2011 *Electrochemical Technologies for Energy Storage and Conversion* (Wiley-VCH Verlag GmbH & Co)

[4] Simon P and Gogotsi Y 2008 Materials for electrochemical capacitors *Nature Mater.* **7** 845-854

[5] Choudhury N A, Sampath S and Shukla A K 2009 Hydrogel-polymer electrolytes for electrochemical capacitors: An overview *Ener. Env. Sci.***2**, 55-67

[6] Park M J, Choi I, Hong J and Kim O 2013 Polymer electrolytes integrated with ionic liquids for future electrochemical devices *J. Appl. Polymer Sci.* **129** 2363-76

[7] Meng C, Liu C, Chen L, Hu C and Fan S 2010 Highly Flexible and All-Solid-State Paperlike Polymer Supercapacitors *Nano Lett.* **10** 4025-31

[8] Lei Y, Cheng S, Ding Y, Zhu X, Wang ZL, and Liu M 2011. Hierarchical network architectures of carbon fiber paper supported cobalt oxide nanonet for high-capacity pseudocapacitors. *Nano Lett.* **12** 321-325.

[9] Bose S, Kuila T, Mishra A K, Rajasekar R, Kim N H and Lee J H 2012 Carbon-based nanostructured materials and their composites as supercapacitor electrodes *J. Mat. Chem.* **22**, 767-84

[10] Candelaria S L, Shao Y, Zhou W, Li X, Xiao J, Zhang J G, Wang Y and Liu J 2012 Nanostructured carbon for energy storage and conversion *Nano Energy* **1**, 195-220

[11] Zhang L L and Zhao X S 2009 Carbon-based materials as supercapacitor electrodes *Chem. Soc. Rev.* **38** 2520-31

[12] Azam M A, Fujiwara A and Shimoda T 2013 Significant capacitance performance of vertically aligned single-walled carbon nanotube supercapacitor by varying potassium hydroxide concentration *Int. J. Electrochem. Sci.* **8** 3902-11

[13] Stoller M D, Park S, Yanwu Z, An J and Ruoff R S 2008 Graphene-Based ultracapacitors *Nano Lett.* **8** 3498-502

[14] Zhang H, Cao G, Yang Y and Gu Z 2008 Comparison between electrochemical properties of aligned carbon nanotube array and entangled carbon nanotube electrodes *J. Electrochem. Soc.* **155** 19-22.

[15] Du C, Yeh J, and Pan N 2005 High power density supercapacitors using locally aligned carbon nanotube electrodes *Nanotechnology* **16**(4) 350-53

[16] Xu Y, Lin Z, Huang X, Liu Y, Huang Y and Duan X 2013 Flexible Solid-State Supercapacitors Based on Three-Dimensional Graphene Hydrogel Films *ACS Nano* **7** 4042-49

[17] El-Kady M F, Strong V, Dubin S and Kaner R B 2012 Laser Scribing of High-Performance and Flexible Graphene-Based Electrochemical Capacitors *Science* **335** 1326-30

[18] El-Kady M F and Kaner R B 2013 Scalable fabrication of high-power graphene micro-supercapacitors for flexible and on-chip energy storage *Nature Comm.* **4** 1475

[19] Yu A, Chabot V and Zhang J 2013 *Electrochemical Supercapacitors for Energy Storage and Delivery* ed: CRC Press

[20] Zhou R, Meng C, Zhu F, Li Q, Liu C and Fan S 2010 High-performance supercapacitors using a nanoporous current collector made from super-aligned carbon nanotubes *Nanotechnology* **21** 345701

[21] Mirri F, Ma A W K, Hsu T T, Behabtu N, Eichmann S L, Young C C, Tsentalovich DE and Pasquali M 2012 High-Performance Carbon Nanotube Transparent Conductive Films by Scalable Dip Coating *ACS Nano* **6** 9737-44

[22] Liu J, Notarianni M, Will G., Tiong V T, Wang H, and Motta N 2013 Electrochemically Exfoliated Graphene for Electrode Films: Effect of Graphene Flake Thickness on the Sheet Resistance and Capacitive Properties *Langmuir* **29** 13307-14

[23] Liu J, Galpaya D, Notarianni M, Yan C and Motta N 2013 Graphene-based thin film supercapacitor with graphene oxide as dielectric spacer *Appl. Phys. Lett.* **103** 063108

[24] Kaempgen M, Chan C K, Ma J, Cui Y and Gruner G 2009 Printable Thin Film Supercapacitors Using Single-Walled Carbon Nanotubes *Nano Lett.* **9** 1872-76

[25] Cheng Q, Tang J, Ma J, Zhang H, Shinya N and Qin L 2011 Graphene and vcarbon nanotube composite electrodes for supercapacitors with ultra-high energy density *Phys. Chem. Chem. Phys*. **13** 11615-24

[26] Wang D H, Kyaw A K K, Gupta V, Bazan G C and Heeger A J 2013 Enhanced

efficiency parameters of solution-processable small-molecule solar cells depending on ITO sheet resistance *Adv. Ener. Mat.* **3**(9) 1161-65

[27] Ueki T and Watanabe M 2008 Macromolecules in ionic liquids: Progress, challenges, and opportunities *Macromolecules* **41**(11) 3739-49

[28] Kang Y J, Kang Y J, Chung H, Han C. H. and Kim W 2012 All-solid-state flexible supercapacitors based on papers coated with carbon nanotubes and ionic-liquid-based gel electrolytes *Nanotechnology* **23**(6) 065401

Figure captions

Figure 1. Cartoon of the three devices. (a) D1: CNT films as both electrodes and current collectors; (b) D2: CNT films as current collectors and graphene films as electrodes; (c) D3: Au films as current collectors and graphene films as electrodes.

Figure 2: (a) Photograph of a typical electrode made by transferring a graphene film onto a PEN-supported CNT film; (b) A tilted-view SEM image of the graphene/CNT double layers; (c) A SEM image of a freestanding graphene film peeled off the substrate. CNTs sticking to the graphene film indicate strong binding force between CNTs and graphene sheets; (d) A plane-view image of the CNT film.

Figure 3: (a) and (b) CV curves for D1 and D2 devices measured at different scan rates, respectively; (c) and (d) Galvanostatic charge-discharge curves of D1 and D2 devices measured at different current densities, respectively.

Figure 4: (a) Nyquist impedance plots measured from 0.05 Hz to 1 MHz for the three devices; (b) Dependence of phase angle change against frequency for the three devices; (c) Specific areal capacitance extracted from the CV curves. The plots of specific mass capacitance against scan rate for the three devices are shown in (d).

Figure 5: (a) Relation between specific capacitance and graphene electrode thickness for D2; (b) Cycling stability of D2 measured by repeatedly galvanostatic charge-discharge.

Figure 6: (a) and (b) Ragone plots (energy density vs power density) for the three devices calculated in terms of volume (cm^3) and weight (kg).

Figures and Captions

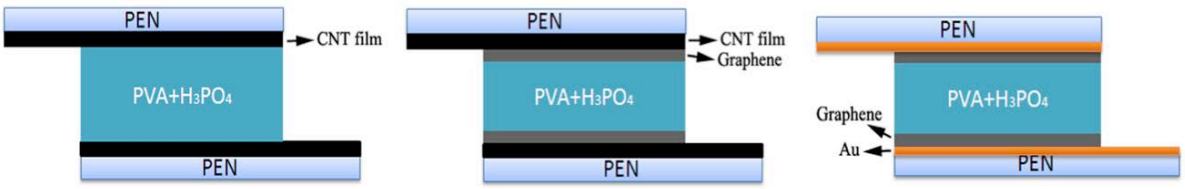

Figure 1. Cartoon of the three devices. (a) D1: CNT films as both electrodes and current collectors; (b) D2: CNT films as current collectors and graphene films as electrodes; (c) D3: Au films as current collectors and graphene films as electrodes.

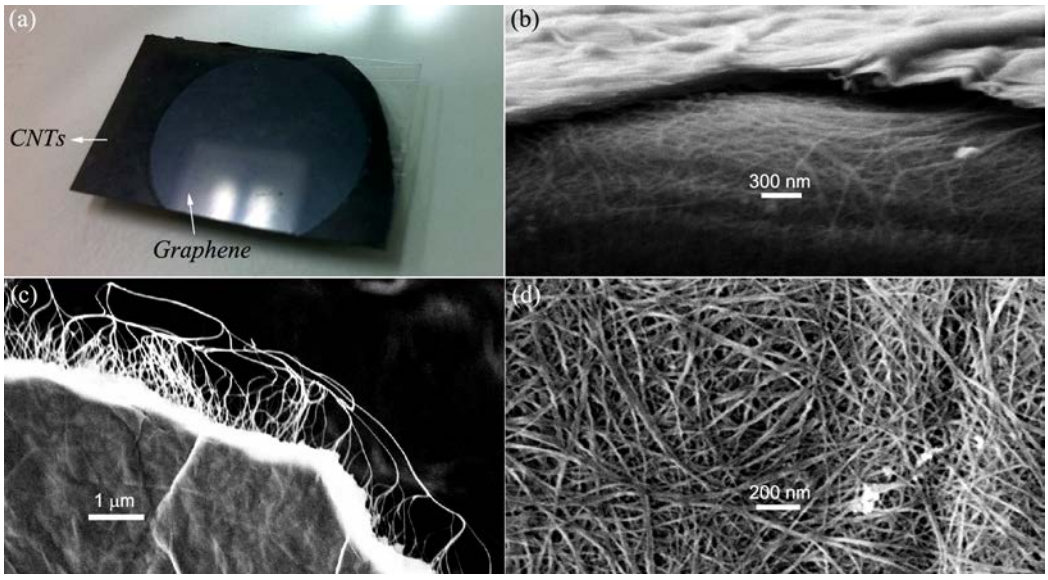

Figure 2: (a) Photograph of a typical electrode made by transferring a graphene film onto a PEN-supported CNT film; (b) A tilted-view SEM image of the graphene/CNT double layers; (c) A SEM image of a freestanding graphene film peeled off the substrate. CNTs sticking to the graphene film indicate strong binding force between CNTs and graphene sheets; (d) A plane-view image of the CNT film.

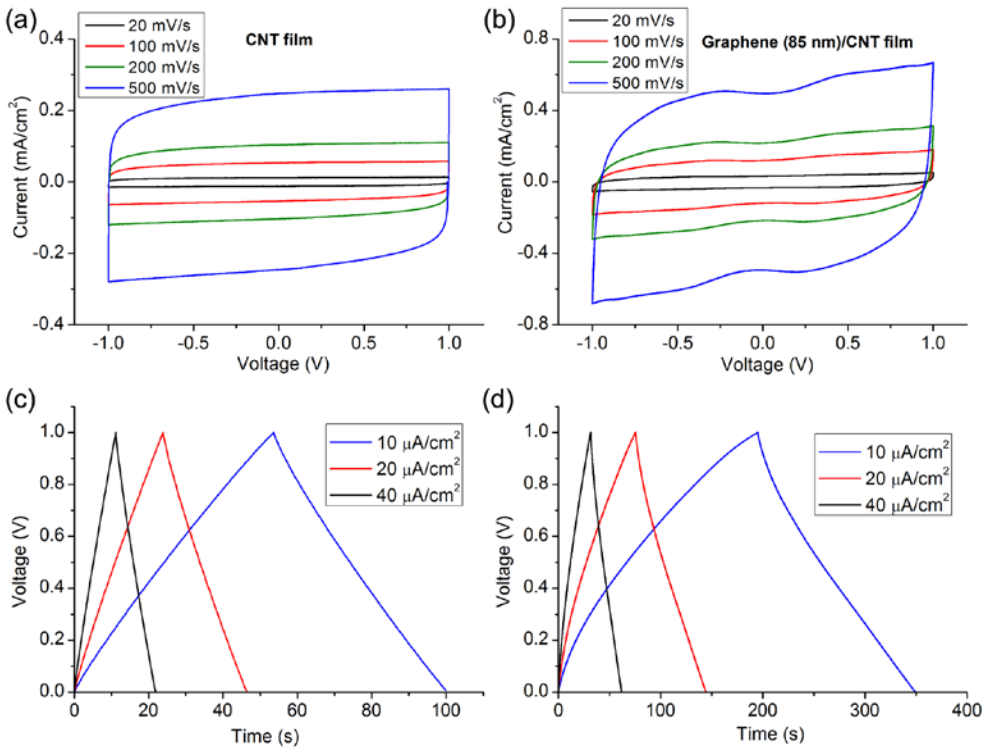

407

408 **Figure 3:** (a) and (b) CV curves for D1 and D2 devices measured at different scan rates,

409 respectively; (c) and (d) Galvanostatic charge-discharge curves of D1 and D2 devices

410 measured at different current densities, respectively.

411

412

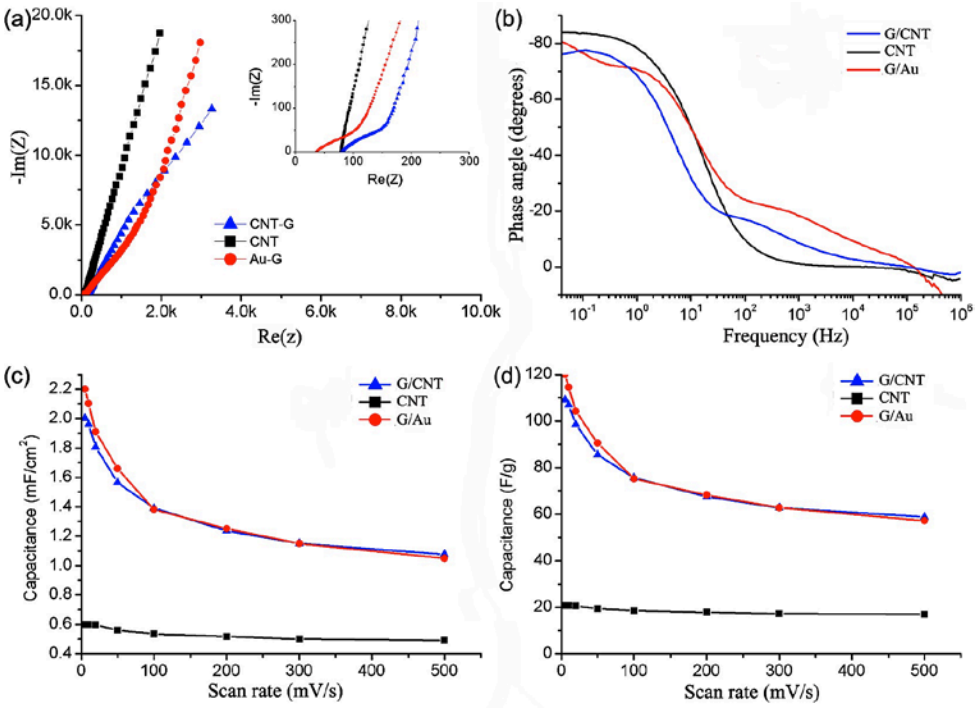

413

414 **Figure 4:** (a) Nyquist impedance plots measured from 0.05 Hz to 1 MHz for the three
415 devices; (b) Dependence of phase angle change against frequency for the three devices;
416 (c) Specific areal capacitance extracted from the CV curves. The plots of specific mass
417 capacitance against scan rate for the three devices are shown in (d).

418

419

420

421

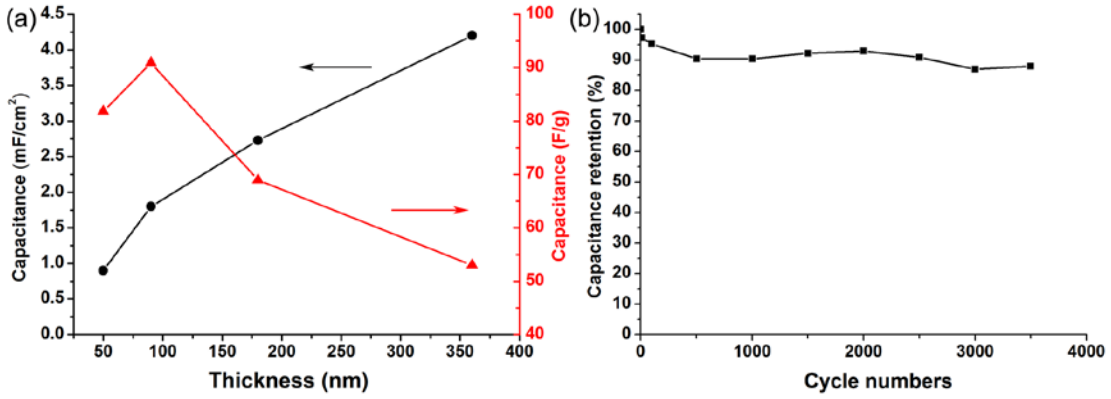

Figure 5: (a) Relation between specific capacitance and graphene electrode thickness for D2; (b) Cycling stability of D2 measured by repeatedly galvanostatic charge-discharge.

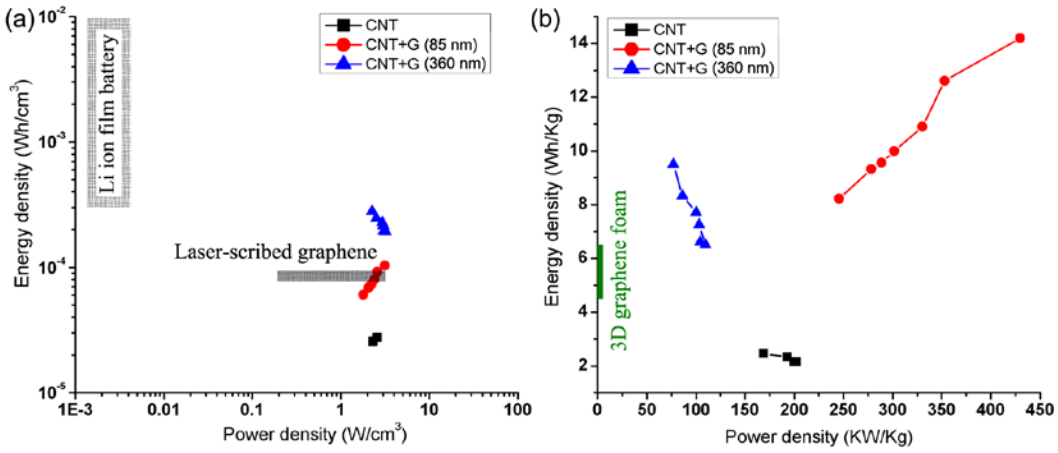

Figure 6: (a) and (b) Ragone plots (energy density vs power density) for the three devices calculated in terms of volume (cm^3) and weight (kg).

Supporting Information

Graphene-based supercapacitor with carbon nanotube film as highly efficient current collector

Marco Notarianni[1], Jinzhang Liu[1], Francesca Mirri[2], Matteo Pasquali[2] and Nunzio Motta[1]

[1]Institute for Future Environments and School of Chemistry, Physics, and Mechanical Engineering, Queensland University of Technology, Brisbane, 4001 QLD, Australia

[2]Department of Chemical and Biomolecular Engineering, The Smalley Institute for Nanoscale Science and Technology, Rice University, 6100 Main Street, Houston, Texas 77005, United States

1. Raman analysis

Figure S1 shows the Raman spectrum (Reinshaw *InVia*) of the DWCNT film measured using the 534 nm laser source. The G band Raman mode at 1593 cm^{-1} corresponds to the tangential movement of atoms on the nanotube surface. The D band, which is observed at 1345 cm^{-1}, is related to defects and disorder.

Raman analysis of the graphene film has been reported previously [1]. The intensity ratio I_D/I_G of graphene can be used to asset the quality. In this regard, our electrochemically produced graphene sheets have less defects and higher quality than GO made by the Hummer's method.

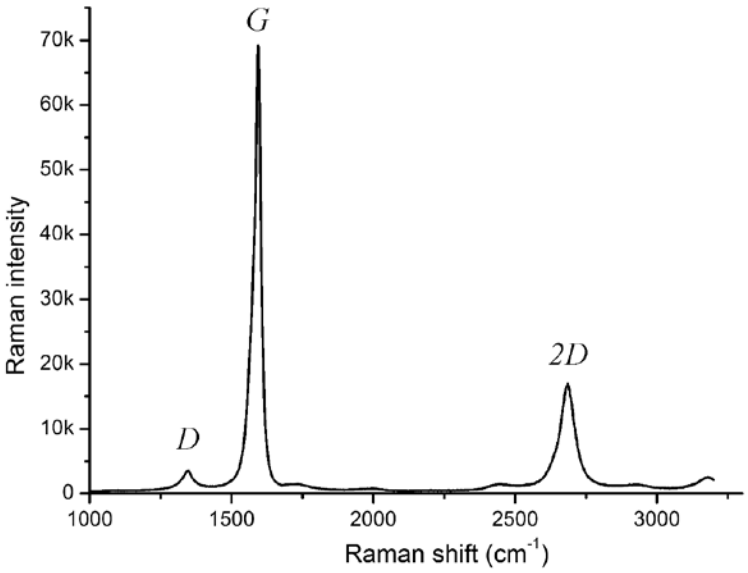

Figure S1: Raman spectrum of a DWCNT film.

2. Strong adhesion between CNTs and graphene sheets

The carbon-nanomaterial-coated plastic substrate was cut to observe the interface between the CNT film and graphene film. The SEM image in figure S2 shows that the graphene film was separated at the edge from the CNT film base due to blade cutting. However those CNTs linking to the bottom face of the graphene film indicate a strong binding force between CNTs and graphene sheets.

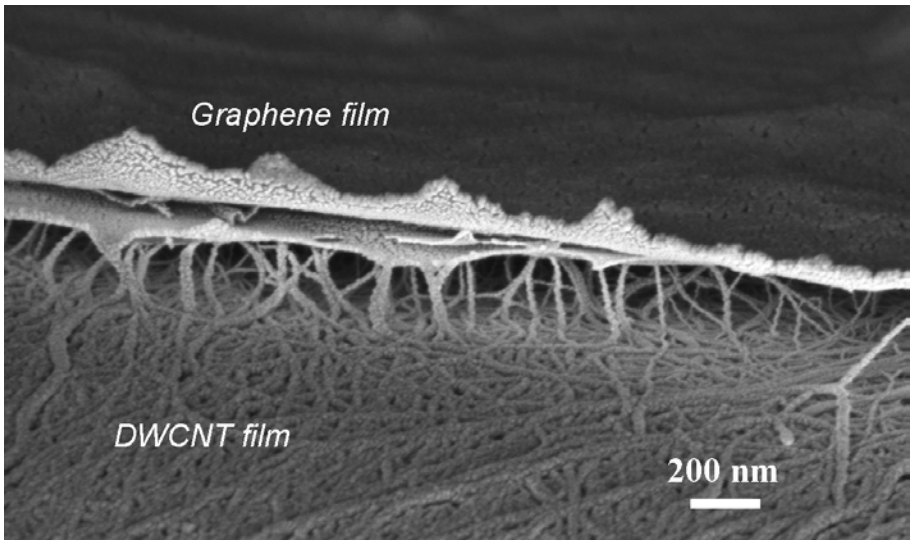

Figure S2: SEM image showing the interface between CNT and graphene films. Strong binding force between CNTs and graphene sheets makes the graphene film attach to the CNT film. The nanoparticle feature is caused by the deposition of Au layer for SEM imaging.

3. Determination of the CNTs film thickness

The film thickness was determined by the Beer-Lambert law: $T = e^{-\alpha h}$, where α is the extinction coefficient, T is the optical transmittance and h is the film thickness. The extinction coefficient α was found to be 0.0054 nm^{-1} by measuring h and T for several films by Atomic Force Microscopy [AFM (Digital Instrument Nanoscope IIIA Atomic force microscope)] and UV-vis spectrometry (Shimadzu UV-1800).

4. Device Performance Calculations

The CV curves are measured in the voltage range of -1 V to +1 V. By treating the graphene supercapacitor as a RC circuit (figure S3), the total current through the

capacitor is $I = C \times dV/dt + V/R$, where *dV/dt* is the voltage scan speed. At V=0, $I_0 = C \times dV/dt$. Hence the capacitance can be obtained as $C=I_0/(dV/dt)$.

To calculate the capacitance using galvanostatic CD curves, the current I and the slope of the discharge curve, *dV/dt*, are used: $C=I/(dV/dt)$. Note that the capacitance range calculated from the CD curves is similar to that from the CV curves.

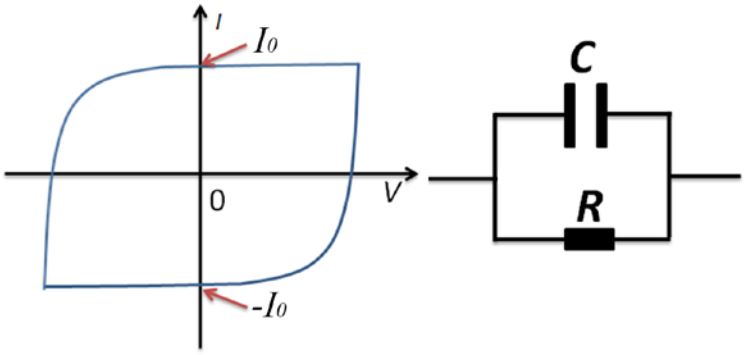

Figure S3: The use of CV curve to deduce the capacitance, by taking the capacitor as a RC circuit.

The power of a single supercapaictor is calculated from the galvanostatic curves at different charge/discharge current densities using the following formula:

$$P = (\Delta V)^2/4R_{ESR}Ad \qquad (1)$$

Where *P* is the power (W/cm^3), ΔV is the operating window (measured in volts and obtained from the discharge curve excluding the IR drop), *A* is the area and *d* is the thickness of gelled electrolyte layer. R_{ESR} is the internal resistance of the device that can be estimated from the voltage drop at the beginning of the discharge and from the discharge current *I* by $R_{ESR} = V_{drop}/2I$.

494 The energy density of the device is obtained by using Eq. (2):

495 $$E = C \times (\Delta V)^2/(2 \times 3600 \times d) \qquad (2)$$

496 Where E is the energy density in Wh/cm^3, C is the areal capacitance, and d is the gap

497 between two opposite electrodes.

498